Journal of Solid State Chemistry **154,** 535–541 (2000)
doi:10.1006/jssc.2000.8876, available online at http://www.idealibrary.com on IDEAL®

On the Crystal Chemistry and Stability of Sm^{2+} in $SmSO_4$ and Solid Solutions of $M_{1-x}Sm_xSO_4$ (M = Ba, Sr)

P. Mikhail, A. Sieber, T. Samtleben, B. Trusch, T. Lüthi, and J. Hulliger[1]

Department of Chemistry and Biochemistry, University of Berne, Freiestrasse 3, CH-3012 Berne, Switzerland

Received April 4, 2000; in revised form June 20, 2000; accepted July 17, 2000; published online September 30, 2000

Solid solution formation of Sm^{2+} and MSO_4 (M = Sr, Ba) was investigated for syntheses using (i) a LiCl high-temperature solution exposed to a reducing atmosphere and (ii) precipitation reactions at room temperature starting from aqueous solutions of SmI_2 or electrochemically gained Sm^{2+}. In contrast to (ii), present results show that a high-temperature approach (i) yielded only a very low amount of Sm^{2+} in $M_{1-x}Sm_xSO_4$. Formation of a solid solution system ($0<x<1$) was confirmed for $Sr_{1-x}Sm_xSO_4$ and $Ba_{1-x}Sm_xSO_4$ by X-ray powder diffraction analysis and optical lifetime measurements. The unit cell parameters of $Ba_{1-x}Sm_xSO_4$ showed a slight deviation from Vegard's law. Positive and negative deviations are in agreement with results on solid solutions of $Ba_{1-x}Sr_xSO_4$. Compounds obtained by syntheses at room temperature were exposed to annealing at 450 to 850°C using a reducing or oxidizing atmosphere. In this temperature range, $M_{1-x}Sm_xSO_4$ (M = Sr, Ba) decomposed into $Sm_2O_2(SO_4)$ and the corresponding MSO_4. Solid solutions of $M_{1-x}Sm_xSO_4$ (M = Ba, Sr) represent a new system for investigating Sm^{2+} in an oxide environment. There are only a few other oxide host lattices stabilizing divalent samarium. © 2000 Academic Press

Key Words: **solid solution; Sm^{2+}; sulfate; flux growth; electrochemical synthesis.**

1. INTRODUCTION

Luminescence from Ln^{2+} ions in crystals, ceramics, and glasses has attracted much attention over the past 15 years (1). The most studied divalent lanthanide species are Eu^{2+}, Yb^{2+}, and Sm^{2+}. Divalent samarium is an interesting ion for the investigation of spectral hole burning (2–7), excited state absorption (8–10), and laser properties (11, 12). There is also a report on spectroscopic methods for distinguishing between Sm^{3+} and Sm^{2+} (13).

The reduction of Ln^{3+} to Ln^{2+} ions in solid state reactions generally needs a strong reducing agent. Most commonly a H_2/N_2, or a H_2/Ar gas mixture was used. This method is well known for halide containing lattices and oxide glasses (14). An alternative is given by an electrochemical reduction for preparing Sm^{2+} salts (15). Up to now, there are only two examples where a valence change from Sm^{3+} to Sm^{2+} could be achieved simply in air and at high temperature: (i) Solid state reaction (16) and single crystal growth (17) of SrB_4O_7:Sm^{2+} and (ii) solid state reaction of BaB_8O_{13}:Sm^{2+} (18). Other methods used X- or γ-irradiation to yield divalent samarium in $CaSO_4$, leaving a hole trapped in the lattice (19,20). Similarly, $BaSO_4$:Sm^{2+} (21) and $SrBa(SO_4)_2$:Sm^{2+} (22) materials have been produced by exposure to a $Co^{60}\gamma$-source.

A low doping concentration of Sm^{2+} found in single crystals of $SrSO_4$ grown by a flux method prompted us to investigate the possibility of forming solid solutions of the system $M_{1-x}Sm_xSO_4$ (M = Sr, Ba). Arguments of size and charge should allow the Sr-sulfate host to be substituted with Sm^{2+} by a much higher amount than found in first crystal growth experiments ($x \leq 0.0002$). Anticipating that Sm^{2+} might not be stable at high temperature in a LiCl flux, we have applied an electrochemical approach to obtain polycrystalline $SmSO_4$ (15) and $M_{1-x}Sm_xSO_4$ solid solutions (M = Ba, Sr). The system $SmSO_4$ and MSO_4 (M = Sr, Ba) provides one of few materials for studying solid solutions involving *divalent* Sm in oxides. The isostructural compounds MSO_4 (M = Ba, Sr, Sm; also Pb) belong to the space group *Pnma* with $Z = 4$ (15, 23, 24). The metal ions in these crystals are surrounded by 12 oxygen atoms resulting in a site symmetry *m*. The cell dimensions of $SrSO_4$ and $SmSO_4$ are similar (see Table 1); this because of a good agreement of the sizes of Sr^{2+} (1.26 Å, CN:8) and Sm^{2+} (1.27 Å, CN:8) (25).

EXPERIMENTAL

1. Flux Growth of Sm-Doped $SrSO_4$ Crystals

Crystal growth out of the melt does not seem possible due to the decomposition of the sulfate ion and a change of the oxidation state of Sm^{2+} before melting. Using a flux method

[1] To whom correspondence should be addressed. E-mail: juerg.hulliger@iac.unibe.ch.

0022-4596/00 $35.00

TABLE 1
Lattice Parameters of Isostructural Compounds MSO_4 (M = Sr, Sm, Ba, Pb) Belonging to the Space Group *Pnma*

Compounds	Lattice parameters (Å)		
	a	*b*	*c*
$SmSO_4$ (15)	8.45	5.38	6.91
$SmSO_4$[a]	8.426(2)	5.344(2)	6.888(3)
$SrSO_4$ (32)	8.359	5.352	6.866
$SrSO_4$[a]	8.361(3)	5.351(3)	6.867(4)
$BaSO_4$ (24)	8.884	5.457	7.157
$BaSO_4$[a]	8.884(1)	5.4557(5)	7.1578(9)
$PbSO_4$ (24)	8.482	5.398	6.959

[a]Result from the present work.

operating at a temperature of 500–700°C is more likely to yield a Sm^{2+} compound.

We used LiCl to dissolve $SrSO_4$ (26, 27) : 17 mol% $SrSO_4$ powder was mixed with 83 mol% LiCl powder, placed in a glassy carbon crucible. 2 mol% of $SmCl_3$ or $SmI_2(thf)_x$ per Sr were added. $SrSO_4$ seed crystals ($2 \times 2 \times 2$ mm) were introduced to facilitate nucleation. The charge was heated up to ~600°C in an Ar/H_2 (80:20 mol%) flow at 10 ml/min. Crystallization was carried out at a cooling rate of 0.2°C/h down to a temperature of 4°C below the eutectic temperature (524°C) (28). Thereafter, the rate was increased to 60°C/h to cool down to room temperature. The solvent was removed by hot water. Finally, crystals of the size about $4 \times 4 \times 4$ mm featuring optical quality were recovered. Fluorescence spectra (Fig. 2) show unambiguously that trivalent and divalent samarium are coexistent. However, the total level of Sm, determined by inductively coupled plasma optical emission spectroscopy (ICP-OES), was quite low (0.003 to 0.02 mol% Sm). At a lower partial pressure of H_2 in Ar/H_2 of 5–10 mol%, fluorescence lines indicated, that predominantly Sm^{2+} was incorporated into $SrSO_4$, although the total amount of Sm was similarly low. This demonstrates the difficulty of establishing conditions for trapping mainly Sm^{2+}. By adding RbCl and NaF to the LiCl flux, the process temperature could be lowered to about 400°C. Since fluoride fluxes have a stabilizing effect (29) on the divalent state of samarium, one may understand that we could trace lines of divalent samarium at a somewhat higher intensity than found for the LiCl flux. Nevertheless, the total amount of Sm found in all high temperature syntheses was lower than expected for ordinary solid solution formation.

Applied to $BaSO_4$, no Sm^{2+} could be traced in fluorescence spectra measured at 25°C. In order to investigate solid solution formation of MSO_4 (M = Sr, Ba) and $SmSO_4$, we therefore have carried out (i) *electrochemical* experiments and (ii) precipitation reactions using a Sm^{2+} precursor at 25°C.

2. Electrochemical Approach

A two-compartment cell was constructed from (i) a quartz tube (cathode) of a diameter of 14 mm. One end of the tube was tapered to a diameter of a Pt wire (Ø = 0.35 mm). The Pt wire was introduced to contact liquid mercury. (ii) The anode compartment consisted of a Pyrex tube with a diameter of 11 mm, which was butt-sealed with a coarse frit. Therein a Pt wire (Ø = 0.35 mm) coiled into a spiral was in contact with the liquid phase.

With the help of this setup, we could reproduce the results of Asprey *et al.* (15), starting from $Sm_2(SO_4)_3$: 2–4 ml of a 0.02 M solution of $Sm_2(SO_4)_3$ in 0.05 M acetic acid were filled onto the mercury electrode. The anode tube was dipped into this solution. The current density varied between 20 and 40 mA/cm^2 at a voltage between 10 and 12 V. Red $SmSO_4$ is insoluble in water and started to precipitate about 2 min after switching on the electrochemical reaction.

For a preparation of the solid solutions of $M_{1-x}Sm_xSO_4$ soluble M salts were used. The SO_4^{2-} was introduced by adding Na_2SO_4 to precipitate $M_{1-x}Sm_xSO_4$. Different proportions of $SmCl_3 \cdot 6H_2O$ and MCl_2 were dissolved in 2 ml H_2O and 6 mg of 96% acetic acid was added. This solution was filled into the electrochemical cell and a voltage of 12 V was applied. Due to the higher electrolyte concentration we obtained a current density between 120 and 360 mA/cm^2. After 1 min the solution turned red, indicative of Sm^{2+}. While waiting for about 4 min or longer, the red color was lost. A fast oxidation of Sm^{2+} was also observed just after interrupting the voltage.

After 1 min of electrochemical reaction, a solution of Na_2SO_4 was injected into the cathode compartment and $M_{1-x}Sm_xSO_4$ (M = Sr, Ba) immediately started to precipitate. The color of the salt differed from red to orange, corresponding to the Sr (Ba) to Sm ratio. Finally, the liquor was removed by a centrifuge. Powders were washed with water and acetone and dried in vacuum (T = 25°C). Stored in an exsiccator, these powders were stable for several months.

Due to the higher oxidation ability in acidic aqueous solution (standard conditions) of the redox couples Cd^{2+}/Cd^0 (−0.4025 V) and Pb^{2+}/Pb^0 (−0.125 V) than Sm^{3+}/Sm^{2+} (−1.55 V), an electrochemical synthesis of solid solutions of MSO_4 (M = Cd, Pb) and $SmSO_4$ was not possible.

An alternative preparation of $M_{1-x}Sm_xSO_4$ was achieved using SmI_2, one of the only Sm(II) chemicals commercially available (14). In this case MCl_2 or MBr_2 was dissolved in water together with SmI_2. Previously Ar was bubbled through the solvent, in order to reduce the oxidation power of the water solution. As described above, SO_4^{2-} was introduced by adding a solution of Na_2SO_4. By this second route, we have also obtained $M_{1-x}Sm_xSO_4$ (M = Sr, Ba). It is interesting to notice that experiments

using Ca^{2+}, Cd^{2+}, and Pb^{2+} did not yield any Sm^{2+} precipitates.

3. *Powder Diffraction Analysis and Luminescence Properties*

Solid solution formation was investigated by X-ray diffraction analysis and optical spectroscopy. Diffraction intensities of powder samples ($Sr_{1-x}Sm_xSO_4$, $Ba_{1-x}Sm_xSO_4$; $0 \le x \le 1$) were collected at room temperature using a high resolution STOE diffractometer (Ge monochromator, $\lambda(CuK\alpha_1) = 1.54$ Å) (sampling: $2\theta = 10^\circ$ to $2\theta = 90^\circ$). For cell refinements, the powder diffraction profile was recorded by step-scanning with an increment of 0.1° and a counting time of 5 s/step. The background was subtracted manually. All cell refinements are based on an orthorhombic structure model (space group *Pnma*) by using the STOE $WinX^{POW}$ program.

Emission and excitation spectra were observed at room temperature. Excitation spectra were measured in the range from 200 to 600 nm by recording the luminescence of the transition $^5D_0 \rightarrow {}^7F_0$ of Sm^{2+} at 681.9 nm ($BaSO_4$) and 683.2 nm ($SrSO_4$), respectively. Excitation spectra were obtained by a Spex fluoromax spectrofluorometer. Fluorescence was excited by a 488-nm Ar^+ laser and recorded from 550 to 775 nm by a Spex 1403 spectrometer with a spectral resolution of 0.2 cm^{-1}.

RESULTS AND DISCUSSION

1. *Solid Solutions*

X-ray diffraction data of all compounds in the series $Ba_{1-x}Sm_xSO_4$ and $Sr_{1-x}Sm_xSO_4$ ($0 \le x \le 1$) showed sharp lines that could be indexed on the base of orthorhombic symmetry.

$Ba_{1-x}Sm_xSO_4$. Lattice parameters were fitted for different molar ratios of Ba and Sm. In Fig. 1, lattice parameters a, b, and c are plotted versus mol% of $SmSO_4$. The molar fractions of samples were determined by electron microprobe analysis up to minimal error of ± 0.12 mol% and a maximal error of ± 1.26 mol%. All data given in Fig. 1 indicate that solid solution formation is possible for $0 < x < 1$. Relatively small deviations from Vegard's law (30) indicate a nonideal solid solution. A similar behavior was reported for other binary sulfate systems (31): The negative deviations for the *a*- and *c*- axis and the positive deviations for the b- axis are in agreement with observations for $Ba_{1-x}Sr_xSO_4$ (32). For this system the following details have been reported (32): Ba, Sr, S, and half of the O atoms are lying on mirror planes perpendicular to the *b*- axis. In plane, Ba and Sr pack more densely than perpendicular to the mirror plane.

$Sr_{1-x}Sm_xSO_4$. Since the lattice parameters of $SmSO_4$ and $SrSO_4$ are very similar (Table 1), calculated unit cell parameters of $Sr_{1-x}Sm_xSO_4$ ($0 < x < 1$) made it more difficult to find a significant relation between the change of the composition and the variation of the lattice parameters. However, the parameters of the mixed crystals lay in between the values of $SrSO_4$ and $SmSO_4$.

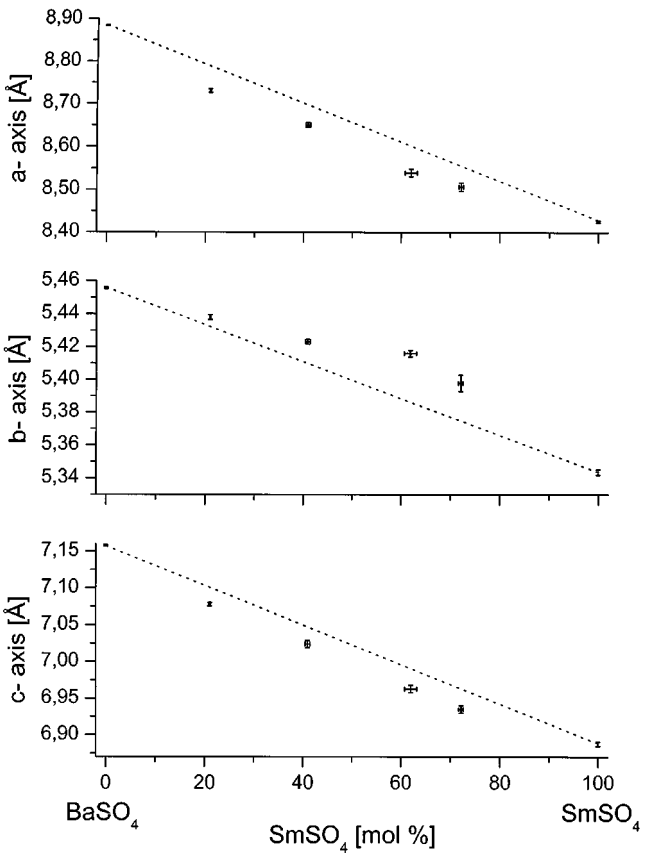

FIG. 1. Lattice parameters *a*, *b*, and *c* of the system $Ba_{1-x}Sm_xSO_4$ fitted to X-ray powder diffraction data.

As mentioned above, trials for obtaining a solid solution of MSO_4 (M = Ca, Cd, Pb) and $SmSO_4$ ended with no success. This might be due to the fact that $CaSO_4$ and $CdSO_4$ crystallize in space groups other than $SmSO_4$ and that the higher oxidation ability of the redox couples Pb^{2+}/Pb^0 than Sm^{3+}/Sm^{2+} may lead to a reoxidation of Sm^{2+} before precipitation can occur.

2. *Optical Properties*

Flux grown crystals of $SrSO_4$:Sm (Fig. 2): Relatively sharp fluorescence lines were observed around 683 nm (14640 cm^{-1}), 697 nm (14350 cm^{-1}), 725 nm (13790 cm^{-1}), 764 nm (13090 cm^{-1}), which are attributed to the $^5D_0 \rightarrow {}^7F_{0,1,2,3}$ transitions of the Sm^{2+} ion. Broad bands observed around 17,860 cm^{-1} (560 nm), 16,800 cm^{-1} (595 nm), and 15,625 cm^{-1} (640 nm), are due to the

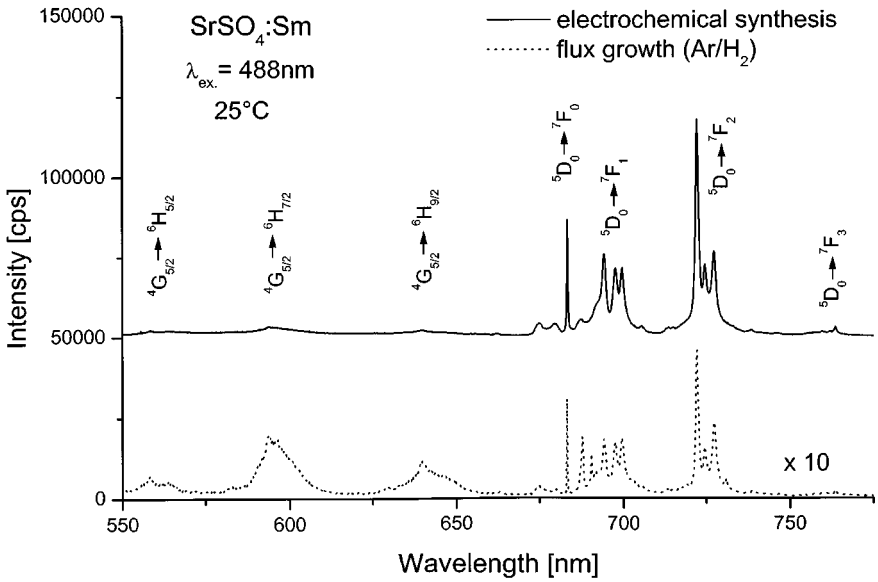

FIG. 2. Fluorescence spectra of Sm in (····) a crystal of $SrSO_4$ grown by flux method in an Ar/H_2 (80:20 mol%) atmosphere and (——) powder sample of $SrSO_4$ synthesized by an electrochemical process. All spectra were measured at 25°C. The broad band transitions $^4G_{5/2} \rightarrow {}^6H_J$ belong to trivalent samarium and the narrow lines are attributed to the transitions $^5D_0 \rightarrow {}^7F_J$ of divalent samarium.

$^4G_{5/2} \rightarrow {}^6H_{5/2,7/2,9/2}$ transitions of the Sm^{3+} ion, respectively. The lines of the trivalent Sm are relatively intense when comparing to those of Sm^{2+}.

Sm^{2+} emission lines of crystals grown by the flux method or from powders (synthesized electrochemically or from the SmI_2 precursor) (Fig. 2) agree within experimental error. Figure 3 shows the emission lines of $BaSO_4$:Sm. Excitation spectra of $SrSO_4$:Sm and $BaSO_4$:Sm are shown in Fig. 4.

Additionally, we have measured the lifetime of the excited state of Sm^{2+} by observing the decay of the transition $^5D_0 \rightarrow {}^7F_0$. A pulsed excitation was provided by an Ar^+ laser at 488 nm in combination with a mechanical shutter. We obtained a τ_{rad} of 6.9 ms at 683.2 nm for $SrSO_4$ and 9.5 ms at 681.9 nm for $BaSO_4$, each material being doped by < 0.4 mol% Sm (Table 2). By increasing the Sm concentration, the lifetime τ_{rad} of Sm^{2+} decreased as known for, e.g.,

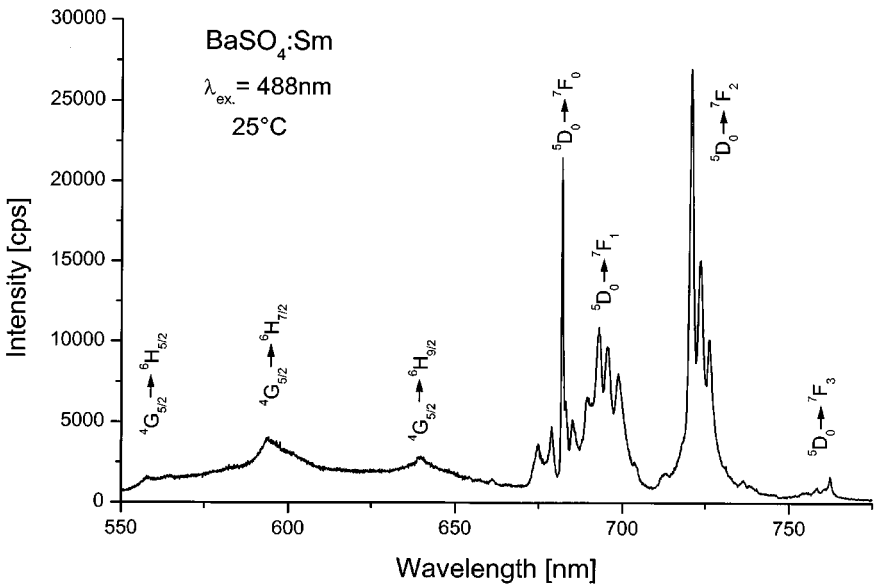

FIG. 3. Fluorescence spectrum of Sm in a powder sample of $BaSO_4$ synthesized by an electrochemical reaction.

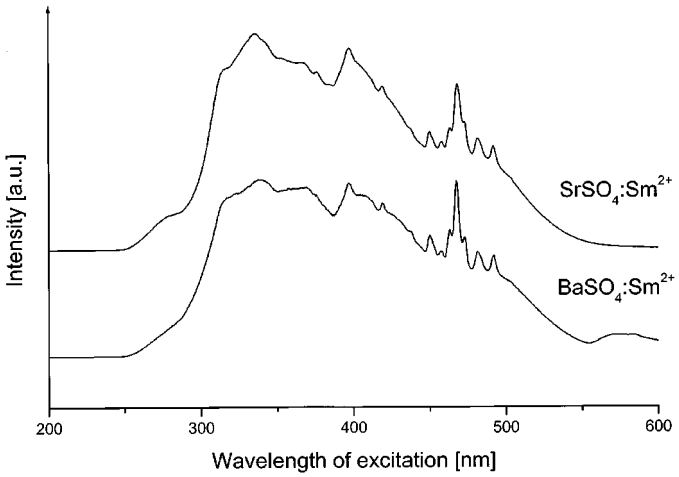

FIG. 4. Excitation spectra (25°C) of Sm^{2+} in $SrSO_4$ and $BaSO_4$ by observing the luminescence of the transition $^5D_0 \rightarrow {}^7F_0$ at $\lambda_{em.} = 681.9$ nm ($BaSO_4:Sm^{2+}$) and $\lambda_{em.} = 683.2$ nm ($SrSO_4:Sm^{2+}$).

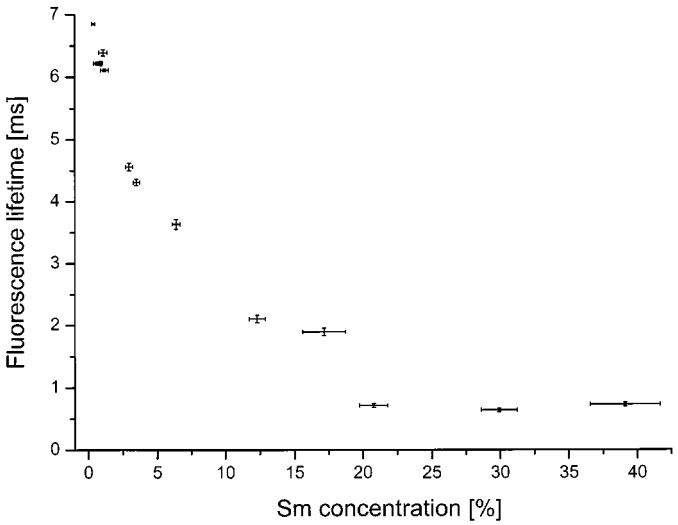

FIG. 5. Fluorescence lifetime of Sm^{2+} vs its concentration in $Sr_{1-x}Sm_xSO_4$ at 25°C.

Nd^{3+} incorporated in different hosts (33, 34, 35). A similar behavior was found for $SrSO_4$ and $BaSO_4$: Fig. 5 shows the fluorescence lifetime versus the Sm concentration in a $SrSO_4$ matrix. For samples with a Sm concentration of < 1.2 mol%, a first-order exponential fit described the luminescence decay quite well. For a higher amount of Sm, significant deviations were found if fitting decay data to a single exponential function. The fluorescence intensity of samples with a Sm level larger than 50 mol% did not allow to measure τ_{rad}. Results in Fig. 5 indicate that there are processes other than simple radiative decay involved being favored by a solid solution system.

In all of these lattices a small amount of Sm^{3+} was incorporated. For Sm^{3+}, we measured the lifetime for the transition $^4G_{5/2} \rightarrow {}^6H_{7/2}$:$SrSO_4$:3.1 ms; $BaSO_4$:4.3 ms (see Table 2).

As a result of X-ray data and lifetime measurements, we conclude that our products obtained by application of an electrochemical potential or reactions using SmI_2 represent *solid solutions.*

TABLE 2
Lifetimes τ_{rad} of Sm^{2+} and Sm^{3+} Incorporated in the Lattice $SrSO_4$ and $BaSO_4$, Respectively

	Lifetime τ_{rad} (ms)	
Lattice	Sm^{2+}	Sm^{3+}
$SrSO_4$	6.9	3.1
$BaSO_4$	9.5	4.3

Note. Lifetime experiments for Sm^{2+} (25°C) were carried out for powder samples containing ~ 0.4 mol% Sm. For measurements of τ_{rad} of Sm^{3+} in $SrSO_4$ we used a single crystal doped with 0.003 mol% Sm.

3. *Thermal Instability of $M_{1-x}Sm_xSO_4$*

To clarify why extended solid solution formation was not possible at a temperature above about 400°C, we have investigated the stability of polycrystalline $Sr_{1-x}Sm_xSO_4$ at temperatures up to 450°C and different atmospheres (air, Ar, or Ar/H_2).

In such experiments, the color (varying from red to orange) changed to pale yellow by heating for 30 min up to 450°C. This was observed for all samples exposed to atmospheres mentioned above. Before heating, initial samples showed a sharp powder diffraction pattern of $Sr_{1-x}Sm_xSO_4$ (Fig. 6B). This pattern disappeared for annealed samples. Instead there were only a few broad reflexes, which could not be indexed (Fig. 6C). Materials heated up to about 450°C seem to be partially amorphous. To complete the reactions, we have heated samples for 10 h at 850°C in air (Fig. 6D). After this treatment lines of $SrSO_4$ appeared. Additional peaks could be fitted to data of $Sm_2O_2(SO_4)$ (36, 37), although agreement was not absolutely complete. Electron microprobe analysis and thermogravimetry indicates that during the heating procedure sulfur is lost as SO_2.

Applied to $Ba_{1-x}Sm_xSO_4$ we have obtained the pattern of $BaSO_4$ and again lines attributed to $Sm_2O_2(SO_4)$. Segregation into $Sm_2O_2(SO_4)$ is supported by the fact, that independent of starting from the Sr or Ba compound, we obtained the same X-ray pattern of $Sm_2O_2(SO_4)$. A temperature of 900°C for preparing the $Sm_2O_2(SO_4)$ phase (36) is close to our final annealing temperature.

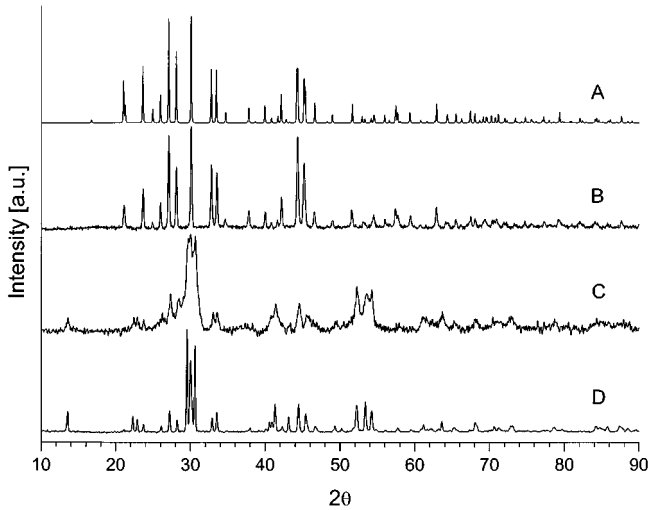

FIG. 6. (A) Calculated powder diffraction pattern for $SmSO_4$. (B) Diffraction pattern of $Sr_{1-x}Sm_xSO_4$ ($x = 0.53$) before annealing; (C) after heating for 30 min at 450°C; (D) after annealing for another 12 h at 850°C in air.

Present results indicate that the stability of divalent Sm in sulfate lattices is not given for temperatures higher than 450°C, even in a nonoxidizing atmosphere. This means that flux growth at 400 to 600°C may well yield only a *small* amount of divalent samarium in $M_{1-x}Sm_xSO_4$ (M = Sr, Ba) as found at the beginning of our work.

CONCLUSIONS

X-ray powder diffraction and optical spectroscopy confirm that $SmSO_4$ and MSO_4 (M = Sr, Ba; $0 \leq x \leq 1$) form a complete system of solid solutions if prepared at room temperature using either an external potential or a Sm^{2+} precursor. From these and other (17) observations we conclude, that for a significant incorporation of Sm^{2+} into oxide-type solid solutions, fitting of the ionic size into the host site is a critical prerequisite. It seems that the Sr- or Ba-site of a few lattices ($SrSO_4$, $BaSO_4$, SrB_4O_7, BaB_8O_{13}) is particularly suited to accommodating Sm^{2+}. With respect to the thermal stability of the Sm^{2+} state, we can say that, in the case of oxidizing anions (e.g., SO_4^{2-}), a valence change to Sm^{3+} is likely, if compounds are to be synthesized at elevated temperature. On the contrary, in the case of the two borates reported so far (17,18), no oxidation can take place through reduction of anionic species. Furthermore, it is not only the influence of size and temperature which may preclude the existence of Sm^{2+} in solid solutions, reduction of cations (e.g., Pb^{2+}, Cd^{2+}) could also work against compound formation.

In essence, we conclude that there is probably a limited number of *oxide* lattices which allow for solid solution formation with Sm^{2+}, even when using a reducing atmosphere (14). Arguments of size, temperature, and electrochemical potentials seem to be the driving parameters for syntheses attempting optically interesting materials providing Sm^{2+}.

ACKNOWLEDGMENTS

We thank M. Wermuth for his assistance in measuring the time-resolved optical spectroscopy, B. Frey for measuring the X-ray powder diffraction patterns, and the group of Prof. Siegenthaler (Berne) for advice in electrochemistry. We are indebted to the group of Prof. H. Bill (Geneva) for using spectroscopic equipment. This work was supported by the Swiss National Science Foundation (Project 2000-057184.99/1).

REFERENCES

1. W. Xu and J. R. Peterson, *J. Alloys Compd.* **249,** 213 (1997).
2. K. Holliday and U. P. Wild, *in* "Molecular Luminescence Spectroscopy" (S. G. Schulman, Eds.), Vol. 77, p. 149. Wiley, New York, 1993.
3. R. M. Macfarlane and R. M. Shelby, *in* "Spectroscopy of Solids Containing Rare Earth Ions" (A. A. Kaplyanskii and R. M. Macfarlane, Eds.), p. 51. Elsevier Science, Amsterdam, 1987.
4. K. K. Rebane and L. A. Rebane, *in* "Persistent Spectral Hole-Burning: Science and Applications" (W. E. Moerner, Ed.), Sect. 2.8. Springer-Verlag, Berlin, 1988.
5. A. Winnacker, R. M. Shelby, and R. M. Macfarlane, *Opt. Lett.* **10,** 350 (1985).
6. R. Jaaniso and H. Bill, *Europhys. Lett.* **16,** 569 (1991).
7. P. Mikhail, M. Schnieper, H. Bill, and J. Hulliger, *Phys. Stat. Sol.* (b) **215,** R17 (1999).
8. S. A. Payne, C. D. Marshall, A. Bayramian, and J. K. Lawson, *Proc. SPIE-Int. Soc. Opt. Eng.* **3176,** 68 (1997).
9. J. K. Lawson and S. A. Payne, *J. Opt. Soc. Am. B* **8,** 1404 (1991).
10. S. A. Payne, L. L. Chase, W. F. Krupke, and L. A. Boatner, *J. Chem. Phys.* **88,** 6751 (1988).
11. P. P. Sorokin, M. J. Stevenson, J. R. Lankard, and G. D. Pettit, *Phys. Rev.* **127,** 503 (1962).
12. P. P. Sorokin and M. J. Stevenson, *IBM J. Res. Dev.* **5,** 56 (1961).
13. P. Mikhail, J. Hulliger, and K. Ramseyer, *Solid State Commun.* **112,** 483 (1999).
14. P. Mikhail and J. Hulliger, *Commun. Inorg. Chem.* **21,** 263 (1999).
15. L. B. Asprey, F. H. Ellinger, and E. Staritzky, *Proc. Rare Earth Res.* **II,** 11 (1964).
16. Z. Pei, Q. Su, and J. Zhang, *J. Alloys Compd.* **198,** 51 (1993).
17. P. Mikhail, J. Hulliger, M. Schnieper, and H. Bill, *J. Mater. Chem.* **10,** 987 (2000).
18. Q. Zeng, Z. Pei, Q. Su, and S. Lu, *J. Lumin.* **82,** 241 (1999).
19. R. L. Calvert and R. J. Danby, *Phys. Stat. Sol.* (a) **83,** 597 (1984).
20. R. J. Danby, K. Holliday, and N. B. Manson, *J. Lumin.* **42,** 83 (1988).
21. S. Chen, C. Qi, T. Wu, F. Dai, P. Qiu, and F. Gan, *Guangxue Xuebao* **22,** 112 (1992).
22. S. Chen, C. Qi, T. Wu, P. Qiu, F. Dai, and F. Gan, *Zhongguo Jiguang* **19,** 132 (1992).
23. D. Garske and D. R. Peacor, *Z. Kristallogr.* **121,** 204 (1965).
24. M. Miyake, I. Minato, H. Morikawa, and S. Iwai, *Am. Miner.* **63,** 506 (1978).
25. R. D. Shannon, *Acta Crystllogr. A* **32,** 751 (1976).
26. A. Packter and B. N. Roy, *Krist. Tech.* **6,** 39 (1971).
27. K. T. Wilke, *Ber. Geolog. Ges.* **7,** 500 (1962).
28. E. M. Levin, C. R. Robbins, and H. F. McMurdie, *in* "Phase Diagrams for Ceramists," Vol. 1, p. 497 (Fig. 1800). American Ceramic Society, Columbus, OH, 1964.

29. J. W. M. Verwey, G. J. Dirksen, and G. Blasse, *J. Phys. Chem. Solids* **53,** 367, (1992).
30. A. R. West, *in* "Solid State Chemistry and Its Applications" (A. R. West, Ed.), p. 366. Wiley, Chichester, 1984.
31. J. C. Butler and C. A. Sorrel, *High Temp. Sci.* **4,** 128 (1972).
32. E. Goldish, *Powder Diffr.* **4,** 214 (1989).
33. R. C. Powell, *in* "Physics of Solid-State Laser Materials" (G. W. F. Drake, Ed.), Chap. 8. Springer-Verlag, New York, 1998.
34. H. G. Danielmeyer, M. Blatte, and P. Balmer, *Appl. Phys.* **1,** 269 (1973).
35. F. Mougel, G. Aka, A. Kahn-Harari, H. Hubert, J. M. Benitez, and D. Vivien, *Opt. Mater.* **8,** 161 (1997).
36. A. A. Grizik, N. G. Abdullina, and N. M. Garifdzhanova, *Russ. J. Inorg. Chem.* **18,** 313 (1973).
37. S. Zhukov, A. Yatsenko, V. Chernyshev, V. Trunov, E. Tserkovnaya, O. Antson, J. Hölsä, P. Baulés, and H. Schenk, *Mater. Res. Bull.* **32,** 43 (1997).